HHS Public Access

Author manuscript

Acta Biomater. Author manuscript; available in PMC 2019 October 01.

Published in final edited form as:

Acta Biomater. 2018 October 01; 79: 253–264. doi:10.1016/j.actbio.2018.08.016.

Graft-specific immune tolerance is determined by residual antigenicity of xenogeneic extracellular matrix scaffolds

Ailsa J. Dalgliesh[a,b], **Mojtaba Parvizi**[b], **Manuela Lopera-Higuita**[b], **Jeny Shklover**[a], and **Leigh G. Griffiths**[b,*]

[a]Department of Veterinary Medicine: Medicine and Epidemiology, University of California, Davis, One Shields Avenue, Davis, CA 95616, USA

[b]Department of Cardiovascular Diseases, Mayo Clinic, 200 First Street SW, Rochester, MN 55905, USA

Abstract

Antigenicity remains the primary barrier towards expanding the use of unfixed xenogeneic biomaterials in clinical applications. An unfixed xenogeneic biomaterial devoid of antigenicity, with maintained structural and mechanical integrity, has potential to overcome the limitations of current clinically utilized glutaraldehyde-fixed xenogeneic biomaterials, such as heart valve bioprostheses. Unfortunately, the threshold level of residual antigenicity necessary to overcome graft-specific immune responses in unfixed xenogeneic tissue has yet to be determined. Furthermore, little information is known regarding the extent to which *in vitro* disruption of native ECM properties, resulting from decellularization or antigen removal procedures, are tolerated following *in vivo* implantation. This manuscript demonstrates that humoral adaptive immune responses are more sensitive to residual xenogeneic biomaterial antigen content than are cell-mediated adaptive responses. Critically, the threshold for tolerable residual antigenicity is identified, with removal of ≥92% of lipophilic antigens required to reduce adaptive immune responses to levels equivalent to glutaraldehyde fixed tissue. Finally, the results demonstrated that the innate immune system tolerates minor changes in protein organization provided that molecular structure is maintained. Antigen removed xenogeneic biomaterials achieving these *in vitro* success criteria induce *in vivo* adaptive and innate tolerance, while modulating pro-regenerative constructive remodeling.

Keywords

Antigenicity; Immune response; Bovine pericardium

*Corresponding author at: Department of Cardiovascular Diseases, Mayo Clinic, 200 First Street SW, Stabile 4-58, Rochester, MN 55905, USA.

Conflict of Interest

The authors report no conflicts of interest.

Appendix A. Supplementary data

Supplementary data associated with this article can be found, in the online version, at https://doi.org/10.1016/j.actbio.2018.08.016.

1. Introduction

Prevalence of heart valve disease is approximately 2.5% in the United States, resulting in 100,000 heart valve replacements annually [1]. Animal derived xenogeneic “tissue” valves are commonly utilized for heart valve replacement due to their superior hemodynamics and avoidance of life-long anticoagulation [1,2]. In an attempt to mask tissue antigenicity, xenogeneic ‘‘tissue” valves are currently subjected to glutaraldehyde fixation prior to implantation. However, recent studies have demonstrated that masking of antigenicity is incomplete following glutaraldehyde fixation, resulting in chronic graft-specific immune response which limits valve life expectancy [3–5]. Additionally, glutaraldehyde fixation renders the prosthesis incompatible with recipient cellular repopulation, remodeling and growth in juvenile patients [6–8]. Consequently, the National Heart, Lung, and Blood Institute recognize the necessity for biomaterials that can overcome the debilitating limitations of current bioprosthetic heart valve replacements [9].

Native tissue extracellular matrix (ECM) structure, composition, and function provides an ideal environment for cell adhesion, migration, differentiation, and proliferation [8,10]. Xenogeneic ECM scaffolds in which native tissue properties are maintained therefore have potential for *in vivo* self-recognition allowing for integration, remodeling, and growth [11–13]. However, tissue antigenicity represents the principal barrier toward use of unfixed xenogeneic ECM biomaterials in clinical practice, due to its ability to stimulate recipient graft-specific adaptive immune responses [5,14,15]. Therefore, the primary goal of antigen removal and decellularization protocols is to remove antigenic components and cellular debris from tissue in a manner that preserves the native ECM microenvironment. Recent advances have demonstrated that antigenicity is not solely confined to tissue cellular elements, and known antigens such as α-gal, as well as unknown antigens, remain even after ‘‘successful” acellularity is achieved [16–18]. Critically, persistent antigenicity of such acellular biomaterials has been shown to stimulate recipient graft-specific adaptive immune response with resultant biomaterial destruction [8,16,19]. Despite these challenges, an unfixed xenogeneic ECM scaffold in which antigenic burden has been eliminated, or significantly reduced, has potential to serve as an ideal heart valve replacement biomaterial.

Even though the field of antigen identification and characterization is still evolving, prior studies have shown that antigens can be broadly categorized based on their solubility [14,20,21]. Such classification schemes may also inform removal strategies, since hydrophilic antigens are more readily solubilized and removed from candidate tissues in aqueous extraction solutions than are lipophilic antigens [22,23]. Furthermore, recent publications have suggested that lipophilic antigens may stimulate a more severe graft-specific immune response than do hydrophilic antigens [13,23]. Although different types of detergents have had varying success at achieving removal of lipophilic antigens, the zwitterionic sulfobetaine family of detergents has shown particular promise in removing these challenging components from candidate xenogeneic tissues [24]. However, the extent to which residual antigenicity must be reduced in order to ameliorate graft-specific immune response towards unfixed xenogeneic ECM scaffolds remains to be determined.

Preservation of native ECM structure, composition and function represents the second critical success criteria in generation of an ideal ECM scaffold [25,26]. However, removal of antigens and/or cells inherently alters the starting tissue. Consequently, reducing tissue antigenicity while preserving native ECM properties represent competing goals in production of ECM scaffolds for clinical application. Previous studies have demonstrated that the specific chemicals utilized in decellularization and antigen removal protocols are paramount in avoiding such off-target ECM damage and therefore in determining ultimate *in vivo* scaffold fate [3,8,13]. The ability of sulfobetaines to solubilize proteins in a nondenaturing manner makes them potentially ideal for such applications [24]. However, the extent to which off-target disruption of native ECM properties is tolerated following *in vivo* implantation remains to be determined.

We hypothesized that the ability of sulfobetaine detergents to reduce ECM scaffold antigenicity while simultaneously maintaining native ECM properties, will prevent recipient graft-specific adaptive and innate immune responses, while fostering non-immune cellular repopulation and tissue integration. In this study, we determined: 1. The sulfobetaine compound and concentration which resulted in maximal reduction in ECM scaffold antigen content, 2. Extent to which preservation of native ECM properties modulates recipient *in vivo* graft-specific innate response, 3. Threshold of *in vitro* residual antigenicity in ECM scaffolds which results in *in vivo* graft-specific adaptive immune tolerance.

2. Materials and methods

All chemicals were purchased from Sigma-Aldrich, St. Louis, MO, USA unless stated otherwise. Expanded methods are available in the Supplementary material.

2.1. Tissue harvest

Bovine pericardium (BP) (Spear Products, Coopersburg, PA) was harvested and epicardial fat removed. The pericardial sac cut into 1 × 16 cm circumferential strips and stored at −80 °C [20].

2.2. Anti-native bovine pericardium serum production

All procedures were performed in accordance with the University of California IACUC Guide for Care and Use of Laboratory Animals [27]. As previously described, anti-BP serum was generated by immunizing New Zealand white rabbits (n = 2) with homogenized BP, with serum collected at 84 days and stored at −80 °C [20].

2.3. Antigen removal

All antigen removal steps were performed in 2 mL of solution at 4 °C, 125 rpm and changed twice daily, unless otherwise stated. Previously frozen BP strips were cut into 1.0 × 1.5 cm pieces and incubated in hydrophile solubilizing solution for 48 h, followed by lipophile solubilizing solution (single sulfobetaine dissolved (w/v) in hydrophile solubilizing solution (Table 1)), for 48 h at RT[20]. Anatomical controls were subjected to 1 min incubation times for hydrophile and lipophile solubilizing solutions, serving as negative controls.

Subsequently, all samples (treatment and control) underwent 24 h of nuclease digestion and 48 h of tris-buffered saline (TBS) washout. All samples were stored at −80 °C [20].

2.4. Residual protein extraction

Following antigen removal, BP scaffolds and controls (see Section 2.3) underwent manual mincing and incubation in protein extraction solution containing 0.1% sodium dodecyl sulfate (SDS) at 1000 rpm, 4 °C for 1 h. Following centrifugation at 17,000g, 4 °C for 30 min supernatant was recovered and designated as residual hydrophilic protein extract. The remaining pellet was washed twice and then incubated in protein extraction solution containing 1% (w/v) SDS at 1400 rpm, 4 °C for 1 h. Following centrifugation, supernatant was recovered and designated as residual lipophilic protein extract. All extracts were stored at −80 °C [20].

2.5. One-dimensional electrophoresis and western blot

Residual protein extracts (see Section 2.4), were assessed for antigenicity using one-dimensional electrophoresis and Western blot. All blots were probed with anti-native BP serum and assessed for IgG positivity using mouse anti-rabbit IgG. (n = 6 per group)[20]. Select antigen removed BP scaffolds (ASB-14 5% and ASB-16 3% respectively) were probed with both murine anti-bovine MHC Class I (Bio-Rad AbD Serotec, Hercules, CA) and anti-Gala1–3Gal b1-(3)4GlcNAc-R (alpha-gal) (Enzo Life Sciences, Farmingdale, NY). Positivity was assessed using goat anti-mouse IgG (Jackson Immuno Research, West Grove, PA). Loading control for all western blot images is protein extraction solution volume, with equal volumes loaded in each well, equating to loading of equal starting tissue mass per well (n = 6 per group) [20,21]. Densitometry was determined using AlphaView image acquisition and analysis software (Alpha Innotech Corp., Santa Clara, CA), with all lanes corrected for background [21]. Antigen removal percentage was calculated as the percent reduction in densitometry between individual AR tissue pieces and their corresponding anatomical control.

2.6. Quantitative biochemistry

For all biochemical analyses, 6 mm discs of native, ASB-14 5%, and ASB-16 3% antigen removed BP scaffolds were weighed, lyophilized for 72 h and re-weighed. Tissue hydration was assessed by calculating the percent loss of sample mass following lyophilization (n = 6 per group per assay) [20]. Samples underwent papain digestion and were assessed for DNA content using QuantiT PicoGreen assay kit (Invitrogen, Paisley, PA) as well as sulfated glycosaminoglycan content using Blyscan GAG assay (Bicolor Ltd., Carrickfergus, UK). Samples underwent oxalic acid digestion and were assessed for elastin content using Fastin Elastin assay (Bicolor Ltd., Carrickfergus, UK). Samples underwent hydrochloric acid digestion and were assessed for collagen content using Hydroxyproline assay (Chondrex Inc., Redmond, WA) (n = 6 per group per assay). Finally, samples underwent digestion in assay buffer and were then assessed for phospholipid content using the phospholipid assay kit (Sigma-Aldrich, St. Louis, MO) (n = 6 per group).

2.7. Differential scanning calorimetry

Collagen denaturation temperature was quantified in lyophilized (see Section 2.6) native, ASB-14 5%, and ASB-16 3% scaffolds using differential scanning calorimetry (DSC). Collagen denaturation temperature was calculated by factoring in sample weight and using the range 220–250 °C to identify temperature at maximal heat flow ($J*g^{-1}* °C$) above baseline (n = 6 per group) [13].

2.8. Uniaxial tensile testing

A custom-made dog bone punch conforming to ASTM standards was used to cut samples with a gauge length of 4 mm and 1 mm width of the dog bone region. Samples were mounted under zero strain and subjected to 5% gauge length/sec constant strain (Instron Model 5565, Canton, MA). Thickness and width were measured from digital images of each sample using ImageJ and incorporated into Instron Bluehill Software in order to calculate Young's Modulus and ultimate tensile stress (n = 6 per group) [20].

2.9. hMSC eGFP transfection

All stem cell associated experiments were performed in accordance with the guidelines and procedures outlined by the Institutional Stem Cell Research Oversight committee. Human mesenchymal stem cells (hMSCs) passaged 3–5 (Lonza, Allendale, NJ) were transduced with enhanced green fluorescent protein (eGFP). The University of California, Davis Vector Core generated the pCCLc-MNDU3-LUC-PGK-EGFP-WPRE lentiviral vector. Recellularization capacity was qualitatively (e.g., morphology of seeded hMSCs) and quantitatively (e.g., Alamar Blue fluorescence intensity) assessed for native, ASB-14 5%, and ASB-16 3% scaffolds.

2.10. Subpannicular scaffold implantation and serum collection

All experimental procedures and protocols were approved by the Mayo Clinic Institutional Animal Care and Use Committee (IACUC) and performed in accordance with guidelines and regulations from the Guide for the Care and Use of Laboratory Animals[27]. New Zealand White rabbits (4 groups, n = 6 per group), underwent subpannicular implantation of native BP, clinical gold standard glutaraldehyde-fixed BP (GFBP), ASB-14 5% or ASB-16 3%. Blood (4 mL) was drawn pre- (0 day) and post (7, 14, 28, 42 and 56 day) implantation, serum isolated and stored at −80 °C. A1.5 cm skin incision was made and subpannicular tissues undermined, creating four 2 × 2 cm pockets, two on either side of the spine. Each rabbit had identical 1 × 1 cm samples from a single group placed in each of the four pockets, and the incision closed routinely. At day 56, all rabbits were euthanized and one sample excised en-bloc and fixed in 10% formalin for 72 h for histology. The other 3 implants were stored at −80 °C for later analysis.

2.11. Recipient graft-specific antibody titre

As previously reported, homogenized native BP was bound in a 96 well plate and probed with rabbit sera collected on days 0, 7, 14, 28, 42, and 56 post-implantation (n = 6 per group, per time point). Linear regression of the reference curve (independent day 0 rabbit serum) was used to determine the temporal graft-specific production of antibodies. Titers from days

14, 28, 42, and 56 were normalized to day 0 for each rabbit to give fold-change relative to baseline for each rabbit/time point [13].

2.12. Histology

For *in vitro* analyses, sample sections were stained with Hematoxylin and Eosin (H&E) Verhoeff van Gieson staining (VVG) and Picro-Sirius Red (PSR). Birefringence of the tissue was imaged from PSR slides using polarized light and percent area of collagen alignment calculated (n = 6 per group). For *ex vivo* analyses, samples were sectioned and paraffin embedded to encompass the middle of each scaffold and all intact tissue layers (n = 6 per group). H&E images (100x) were used for quantification of encapsulation thickness by taking measurements along the subpannicular surface of each scaffold as well as the deep surface of the scaffold, adjacent to the epaxial muscles, and averaging the results.

Paraffin embedded scaffold sections were deparaffinized and antigen retrieval performed with target retrieval solution pH 9 (DAKO, Carpinteria, CA). Endogenous peroxidase was blocked with hydrogen peroxide and non-specific binding blocked with 10% goat serum (SeraCare Life Sciences, Milford, MA). *Ex vivo* sample sections were incubated with primary antibody: mouse anti-rabbit MAC387 (macrophage marker, Abcam) and rabbit anti-rabbit CD3 (T-cell marker). Sections were incubated with secondary antibodies (peroxidase labeled polymer anti-mouse and peroxidase labeled polymer anti-rabbit (DAKO) respectively). Staining was performed with chromogen system 3,30-Diaminobenzidine substrate (DAKO), counterstained in Mayer's Hematoxylin and mounted in Faramount mounting medium (DAKO).

Laminin and Collagen Type IV content and organization were qualitatively assessed in native, ASB-14 5%, and ASB-16 3% scaffolds using immunofluorescence. Deparaffinization was executed on 4 μm scaffold sections and then underwent a 3% peroxidase block in methanol for 15 min at RT and were rinsed with PBST. Sections were then incubated in 10% Normal Donkey Serum and PBST for 30 min at RT. Lastly, samples were incubated in either 1:50 laminin or 1:1000 anti-Col IV in 10% NDS/PBST at 4 °C overnight. Sections were rinsed with PBST and incubated with the secondary antibody in 10% NDS/PBST for 60 min at RT in the dark at a 1:200 dilution. Following secondary antibody incubation, the sections were dehydrated, mounted and imaged using Nikon Eclipse Ni-E microscope (Nikon, Melville, NY).

2.13. Cytotoxicity assessment of antigen removed bovine pericardium

Scaffolds following antigen removal were assessed for residual cytotoxicity and underwent varying washout durations (1, 2, 3, and 5 d) with $n = 4$ per group/time point. The hMSCs were cultured in 96-well plates (Corning, NY) at 30,000 cells/well overnight and media was changed following 24 h. Following 2 h incubation at 37 °C, 5% CO2, washout medium was removed and replaced with a combination of 10 μL AlamarBlue (Invitrogen, Carlsbad, CA) and 100 μL for an additional 1.5 h. Fluorescent intensity was measured using Cytation3 imaging reader (560Ex/590Em).

2.14. Calcification

Sample calcification was determined for native BP, GFBP, ASB-14 5% and ASB-16 3% using calcium detection assay kit (Abcam, Cambridge, UK) (n = 6 per group).

2.15. Blinded veterinary pathology review

A blinded review of H&E slides by a board certified veterinary pathologist categorized the morphological change in bovine pericardium subcutaneous implants in leporine subjects using a semi-quantitative scale (Table 2).

2.16. Statistical analysis

In vitro data were analyzed using one-way analysis of variance (ANOVA) with Tukey HSD *post-hoc* test, unless otherwise stated. ELISA analysis was conducted using repeated measures ANOVA and Tukey-Kramer HSD *post-hoc* analyses on standard least squares means. Data generated from pathology review was analyzed using a Wilcoxon/Kruskal-Wallis Test with Dunn *post-hoc* analysis on non-parametric medians. Parametric data are expressed as mean ± standard deviation (s.d.) and non-parametric data are expressed as median ± interquartile range (IQR). Statistical significance is defined at $p < 0.05$ (See Table 3).

3. Results

3.1. Extent of lipophilic antigen removal is dependent on specific sulfobetaine employed

To determine the most effective sulfobetaine compound for removal of both hydrophilic and lipophilic antigens from bovine pericardium, a phased study design was employed. Phase 1 screening studies were used to determine the effect of 6 different sulfobetaines on residual scaffold antigenicity (Supplementary Fig. 1). Phase 2 studies were then employed to optimize the concentration of those Phase 1 sulfabetaines demonstrating capacity to significantly increase removal of lipophilic antigens. Removal of hydrophilic antigens was unaffected by specific sulfobetaine compound or concentration used ($p > 0.05$) (Fig. 1A). Conversely, removal of lipophilic antigens was significantly different between groups, with ASB-14 or ASB-16 removing significantly more lipophilic antigens than any other sulfobetaine tested ($p < 0.0001$) (Fig. 1B). Both ASB-14 and ASB-16 demonstrated a trend towards increasing removal of lipophilic antigens with increased concentration, although this failed to reach statistical significance ($p > 0.9999$ and $p = 0.4356$ respectively).

For ASB-14 and ASB-16, the effect of concentration on removal of lipophilic antigens from bovine pericardium was further examined. No statistically significant effect of ASB-14 concentration on hydrophilic antigen removal was found ($p > 0.05$). However, all concentrations removed >86%, with concentrations of ≥2% ASB-14 removing >95% of hydrophilic antigens (Fig. 1C). Lipophilic antigen removal increased with increasing concentration of ASB-14, reaching a plateau with 5% ASB-14 (ASB-14 5%) (78.7 ± 2.7% removal) ($p < 0.0001$). No statistically significant effect of ASB-16 concentration on removal of hydrophilic antigens was identified ($p > 0.05$) (Fig. 1D). However, all concentrations removed >90%, with concentrations of ≥ 2% ASB-16 removing > 94% of hydrophilic antigens. A concentration dependent effect of ASB-16 on lipophilic antigen

removal was identified ($p < 0.0001$), which was maximal with 3% ASB-16 (ASB-16 3%) (91.5 ± 3.6% removal) (Fig. 1D).

In both ASB-14 5% and ASB-16 3% treated scaffolds, known antigens such as galactose-alpha-1,3-galactose (α-gal) and major histone complex I (MHCI) were significantly reduced compared to native tissue. Western blots were run on lipophilic and hydrophilic extract from native, ASB-14 5%, and ASB-16 3% scaffolds to assess for residual α-gal (Fig. 1E) and MHCI (Fig. 1H). Use of ASB-14 5% and ASB-16 3% significantly reduced residual α-gal in both the hydrophilic (98% and 99% removal respectively, $p < 0.0001$) and lipophilic (97% and 99% removal respectively, $p < 0.0001$) extracts (Fig. 1F and G respectively) compared to native tissue. Residual MHCI from hydrophilic extract (Fig. 1I) in ASB-14 5% and ASB-16 3% scaffolds was also significantly reduced when compared to native tissue (86% and 95% removal respectively, $p = 0.0014$), as was MHCI in the lipophilic extract (81% and 99% removal respectively, $p = 0.0043$) (Fig. 1J).

3.2. Antigen removal with sulfobetaines preserves native extracellular matrix Structure, composition and function

Since ECM damage has been shown to result in activation of *in vivo* innate immune responses, effect of optimal antigen removal concentrations of ASB-14 5% and ASB-16 3% on resultant ECM scaffold structure, composition and function were examined. No qualitative differences in ECM morphology were observed between native BP and ECM scaffolds generated using ASB-14 5% or ASB-16 3% scaffolds (Fig. 2A). Both sulfobetaines effectively decellularized BP as indicated by elimination of nuclei and nuclei remnants on H&E staining (Fig. 2A). VVG-stained sections demonstrated that elastin and collagen content, and elastin fibril orientation were grossly maintained (Fig. 2A). However, PSR-stained sections demonstrated less clearly defined collagen bundles in ASB-14 5% scaffolds compared to native tissue and ASB-16 3% scaffolds (Fig. 2A).

To further assess removal of cell nuclei and cellular remnants, scaffold DNA content was assessed. Both sulfobetaines removed >97% of native BP DNA (5.6 ± 0.7 μg/mg) ($p < 0.0001$), with residual scaffold DNA contents of 0.11 ± 0.07 μg/mg (ASB-14 5%) and0.04 ± 0.05 μg/mg (ASB-16 5%) (Fig. 2B). Both ASB-14 5%(20.0 ± 10.3 nM/g) and ASB-16 3% (28.72 ± 6.09 nM/g) removed >94% of native BP phosphatidylcholine (476.75 ± 22.03 nM/g) ($p < 0.0001$ and $p < 0.0001$ respectively) (Fig. 2C).

Quantification of scaffold composition was undertaken to assess effect of ASB-14 5% and ASB-16 3% on resultant scaffold biochemical composition. Collagen content (Fig. 2D) and alignment (Fig. 2E) of ASB-14 5% scaffolds (85.34 ± 11.08% and 15.1 ± 0.2% respectively) were significantly increased compared to native tissue(67.0 ± 12.6% and 24.8 ± 2.5% respectively) ($p = 0.0349$ and $p = 0.0047$ respectively), whereas these properties were unchanged in ASB-16 3% scaffolds (74.0 ± 10.4% and 22.6 ± 6.5% respectively) ($p = 0.5539$ and $p = 0.6382$). Furthermore, ASB-14 5% significantly reduced the presence of elastin (1.3 ± 0.7%) (Fig. 2F), and glycosaminoglycan (0.01 ± 0.01%) (Fig. 2G) content compared to native (3.0 ± 0.2% and 0.5 ± 0.3% respectively) ($p = 0.0143$ and $p < 0.0002$ respectively), whereas ASB-16 3% significantly reduced the presence of only glycosaminoglycans (0.03 ± 0.02%) (Fig. 2G) ($p = 0.0005$), while preserving elastin content

(2.1 ± 1.3%) ($p = 0.2467$) (Fig. 2F). There was also no change in the hydration between ASB-14 5%, ASB-16 3% or native scaffolds ($p < 0.05$) (Supplementary Fig. 2). ASB-16 3% scaffolds maintained native collagen IV and laminin content and organization, whereas ASB-14 5% scaffolds exhibited disruption and reduction in content of both of these important basement membrane components (Supplementary Fig. 3).

Mechanical properties of the scaffolds were examined to determine whether use of sulfobetaines preserved scaffold utility as compared to native tissue. Both ultimate tensile strength (Fig. 2H) and Young's modulus (Fig. 2I) were preserved for ASB-14 5% (6.0 ± 0.8 MPa and 12.9 ± 0.9 MPa respectively) and ASB-16 3% (7.0 ± 1.8 MPa and 15.2 ± 2.9 MPa respectively) compared to native BP (6.10 ± 2.09 MPa and 15.9 ± 6.7 MPa respectively) ($p = 0.5190$ and $p = 0.4563$ respectively).

Recellularization capacity was qualitatively (e.g., morphology of seeded hMSCs) and quantitatively (e.g., Alamar Blue fluorescence intensity) assessed for native, ASB-14 5%, and ASB-16 3% scaffolds. There was no qualitative difference in recellularization capacity or cell morphology (Fig. 3A), and no statistical difference in the quantitative cell proliferation between scaffolds and native tissue (Fig. 3B).

3.3. Use of sulfobetaines in antigen removal overcomes graft-specific Cell-Mediated adaptive immune response

The extent to which antigen removal modulates recipient graft-specific cell-mediated immune response was examined. The reduction in antigenicity of ASB-14 5% and ASB-16 3% scaffolds resulted in a marked decrease in the cell-mediated graft-specific immune response compared to native tissue (Fig. 4A). Native, and to a lesser extent, GFBP, scaffolds showed severe small mononuclear cell infiltration. Conversely, ASB-14 5% and ASB-16 3% scaffolds showed minimal to no immune cell presence. CD3 staining demonstrated prominent lymphocyte staining with frequent lymphoid follicle presence for native tissue. GFBP scaffolds also demonstrated frequent lymphocyte presence, although follicle formation was rare. Lymphocytes were completely absent in ASB-14 5% or ASB-16 3% scaffolds (Fig. 4A). Blinded pathologist review of the mixed-inflammatory cell response found both ASB-14 5% and ASB-16 3% scaffolds had no immune cell infiltrate which was significantly less than that for native scaffolds ($p = 0.0313$ and $p = 0.0313$ respectively) (Fig. 4B). Explanted native (0.04 ± 0.02 μg/mg) scaffolds also had significantly more calcium deposition than GFBP(0.02 ± 0.01 μg/mg), ASB-14 5% (0.02 ± 0.01 μg/mg), and ASB-16 3% (0.02 ± 0.01 μg/mg) scaffolds ($p = 0.0177$, $p = 0.0495$, $p = 0.0360$ respectively) (Fig. 4C).

3.4. Threshold of residual antigenicity required to reduce recipient graft-specific humoral adaptive immune response is extremely low

Graft-specific antibody production was examined to determine the sensitivity of the humoral adaptive immune response to residual scaffold antigenicity. Although there was no statistically significant difference in the percentage of hydrophilic antigens removed between scaffolds treated with ASB-14 5% (94.7 ± 2.4%) and ASB-16 3% (95.9 ± 1.8%) ($p = 0.3866$) (Fig. 5A), removal of lipophilic antigens was significantly increased for ASB-16 3%

(91.5 ± 3.6%) scaffolds compared to ASB-14 5% (78.7 ± 2.7%) ($p = 0.0003$) (Fig. 5B). Graft-specific humoral immune response (Fig. 5C) towards ASB-16 3% scaffolds was not significantly different than that towards GFBP ($p = 0.4919$) (Fig. 5D). Conversely, ASB-14 5% scaffold stimulated significantly greater graft-specific antibody production than that towards GFBP ($p = 0.0298$).

3.5. Perturbations in ECM composition and structure are tolerated if macromolecular structure is intact

The extent to which perturbations of native ECM structure, composition and function modulate *in vivo* recipient innate immune and pro-regenerative non-immune responses were investigated. Picrosirius staining and polarized light (Fig. 6A) demonstrates extensive fibrous encapsulation of both native and GFBP scaffolds. Fibrous encapsulation of ASB-14 5% (29.9 ± 17.4 μm) or ASB-16 3% (23.1 ± 9.9 μm) was almost non-existent and significantly less than that of either native (243.2 ± 30.7 μm) or GFBP (167.5 ± 77.8 μm) ($p < 0.0001$) (Fig. 6B). Scaffold fibrosis was closely associated with degree of macrophage presence, which was minimal in ASB-14 5% or ASB-16 3% scaffolds (Fig. 6A), yet substantial in native implants and moderate in GFBP (Fig. 6A). Pathology review identified evidence of significant degeneration and necrosis in both native and GFBP groups ($p = 0.1476$), whereas antigen removed groups showed no evidence of such negative consequences of recipient cellular repopulation events (Fig. 6C) ($p < 0.0001$). Indeed, both ASB-14 5% and ASB-16 3% groups showed evidence of full thickness non-immune cellular repopulation, with complete absence of degeneration and necrosis ($p > 0.9999$) (Fig. 6C). Both antigen removed groups showed a substantial number of non-immune spindle shaped cells had migrated into the center of their respective scaffolds and those cells appeared healthy with normal cell morphology similar to fibrob-lasts (Fig. 6A). Both ASB-14 5% and ASB-16 3% scaffolds demonstrated preservation of native collagen macromolecular structure, as characterized by their collagen denaturation temperature (i.e., differential scanning calorimetry) prior to implantation ($p = 0.3629$) (Fig. 6D). However, following *in vivo* implantation polarized light microscopy (Fig. 6A) demonstrated that collagen in ASB-16 3% scaffolds have reduced collagen polarization and overall scaffold thickness compared to ASB-14 5%, even though there are no differences in innate immune response towards either scaffold type.

4. Discussion

A promising way to circumvent the limitations of current biological heart valves is through use of an un-fixed xenogeneic ECM scaffold, where antigenicity has been substantially reduced or eliminated. Studies from multiple researchers have identified that antigenic components remain in acellular tissues and are associated with detrimental *in vivo* graft-specific immune responses [13,16,17,28]. Furthermore, preservation of native ECM structure, composition and function following antigen removal is critical in successful scaffold generation. Until now, the threshold level of residual antigenicity necessary to overcome the graft-specific immune response has remained elusive. Additionally, the sensitivity of the predominant elements of the adaptive immune system toward residual antigens has not been identified. Here we demonstrated that humoral immune responses are

a more sensitive indicator of recipient graft-specific adaptive response than are cell-mediated responses. We also determined the level of antigenicity equivalent to the clinical gold standard in graft-specific antibody production. Consequently, this study for the first time establishes a threshold for tolerable residual antigenicity in unfixed xenogeneic biomaterials. Additionally, the current work further identified that preservation of ECM protein macromolecular structure is potentially more crucial than individual fiber alignment for avoiding innate immune mediated foreign body response. This work allows for the development of superior unfixed xenogeneic biomaterials capable of avoiding destructive recipient graft-specific immune responses while fostering non-immune cellular repopulation and remodeling.

The challenges inherent in identification of antigenic tissue components limit understanding of recipient graft-specific immune responses. More so, the identities and relative immunogenicity of minor histocompatibility antigens remains largely unexplored [13,17]. Recent *in vivo* studies indicate that lipophilic antigens may engender a greater graft-specific adaptive immune response than hydrophilic antigens [3,13,29]. This dichotomy may result from the fact that majority of lipophilic antigens are membrane associated and thus more readily available for adaptive immune surveillance than are hydrophilic cellular antigens [14,30]. Unfortunately, this concern is compounded by the fact that lipophilic antigens have inherently low solubility in aqueous solutions and are therefore challenging to remove from candidate tissues [23,24,31]. This combination of factors results in lipophilic antigenicity representing a critical impediment in development of an immunologically-acceptable xenogeneic ECM scaffolds.

The ability of detergents to remove lipophilic antigens from candidate xenogeneic biomaterials, while maintaining native ECM structure, composition and function, varies dependent on the mechanism of action of the detergent class and the specific detergent utilized. However, ionic detergents, such as sodium dodecyl sulfate (SDS), have been shown to have surprisingly poor performance in solubilization and removal of lipophilic antigens. This results in persistence of both known (e.g., MHC I) and unknown (i.e., 70% residual antigenicity remaining) lipophilic antigens [3,13,32]. Furthermore, studies have shown SDS to severely denature vital ECM proteins and be toxic to repopulating cells, stimulating recipient innate immune mediated foreign body response [3,10,13,33–35]. Conversely, zwitterionic detergents (e.g., sulfobetaines) are powerful protein solubilizers due to their hydrophilic head and hydrophobic tail [23,24,36]. One particular class of detergents in the sulfobetaine family is the amidosulfobetaine compounds, which were explicitly designed to maximize protein solubilization for isoelectric focusing [24]. Consequently, amidosulfobetaine compounds are capable of maintaining solubility of highly lipophilic proteins even at pH close to their isoelectric point. Amidosulfobetaines have the ideal alkyl tail length (C11-C12), a relatively strong polar head and an amido spacer [22,24]. Combined, these components act to maximize protein solubility and minimize chaotrope interference, allowing them to selectively bind ions [24]. Interestingly, despite documented success in lipophile solubilization for analytical chemistry applications, not all sulfobetaines tested in the current study resulted in reduction of lipophilic tissue antigenicity [24,31,37]. Consequently, we conclude that individual assessment of detergent efficacy in the essential removal of lipophilic antigens from xenogeneic tissue cannot be predicted based on the

solubilization profile determined by analytical proteomics. Upon further investigation, we found a dose-dependent increase in lipophilic antigen removal for the most successful amidosulfobetaines. Lipophilic antigen removal plateaued at 79% removed for ASB-14 at 5% w/v and 92% removed for ASB-16 at 3% w/v. Although neither detergent statistically increased hydrophilic antigen removal compared to no detergent use, the level of hydrophilic antigen removal achieved was greater than any previously reported method for both ASB-14 (95%) and ASB-16 (96%) [13,20,38]. The results of this study demonstrate that although sulfobetaines show great promise in solubilization and subsequent removal of lipophilic antigens from bovine pericardium, the ability of individual sulfobetaines to achieve antigen removal cannot be predicted from their solubilizing profile determined through analytical chemistry.

Although adaptive and innate immune response to whole organ transplantation has been carefully studied, the response to acellular xenogeneic materials has been less thoroughly investigated. Consequently, understanding of this critical aspect of ECM scaffold biology is limited [3]. In the current study, graft-specific immune response was investigated for both the cell-mediated and humoral arms of the adaptive immune system. As expected, recipient response towards native tissue was characterized by intense immune cell presence, with frequent $CD3^+$ T-cell infiltration and lymphoid follicle formation. Surprisingly, despite antigen-masking via glutaraldehyde-fixation, GFBP scaffolds stimulated local $CD3^+$ T-cell infiltration. Lymphocyte infiltration in glutaraldehyde-fixed tissues is not unprecedented and multiple studies have reported similar immune cell infiltration [5,6,29,39]. Glutaraldehyde fixed tissues have been previously demonstrated to leach toxic, unstable glutaraldehyde polymers and aldehyde groups at the implantation site, increasing the probability of tissue calcification [5–7,29,40]. Such toxic damage has been associated with cytotoxic T-cell activation and could account for the signifi-cant lymphocytes presence in GFBP scaffolds explanted in this study. Both ASB-14 5% and ASB-16 3% scaffolds in the current study showed impressive graft-specific cell-mediated responses, with no evidence of local $CD3^+$ T-cell infiltration or follicle formation. The substantial removal of known MHCI antigens by ASB-14 5% (81%) and ASB-16 3% (99%) likely directly contributed to overcoming the cell-mediated immune response compared to native scaffolds[13]. Although this model is not discordant, removal of 85% of agal with ASB-14 5% and 95% with ASB-15 3% provides evidence that these findings have potential to translate to discordant transplantation models and clinical practice. Critically, despite the signifi-cant difference in lipophilic antigen removal between ASB-14 5% and ASB-16 3% scaffolds, cell-mediated adaptive response was indistinguishable between the materials. More so, residual graft-specific humoral responses towards such scaffolds did not appear pathologic, since they were not stimulating any detectable innate (Fig. 6) or adaptive (Fig. 4) immune effector cell recruitment. Consequently, the possibility that such antibodies are involved in tolerance induction requires future investigation. Importantly, the levels of removal of both known and unknown antigens achieved in this work are substantial compared to those previously reported for SDS decellularization, which was only able to achieve removal of 76% MHCI, 86% α-gal, 80% hydrophilic and 37% lipophilic antigens [13,20]. Consequently, both ASB-14 5% and ASB-16 3% scaffolds were equally capable of reducing recipient graft-specific cell-mediated immune response below levels observed for GFBP, suggesting that

both biomaterials may avoid cell-mediated immune destruction following *in vivo* implantation.

Although antigenicity represents a crucial limitation, a threshold level of reduced antigenicity necessary to ameliorate the graft-specific adaptive immune response is yet to be established. Even though the graft-specific cell-mediated immune response was not different between ASB-14 5% and ASB-16 3% scaffolds, important differences in recipient graft-specific humoral immune response were identified. Specifically, graft-specific humoral response towards ASB-16 3% scaffolds was not significantly different than that towards clinical gold standard GFBP scaffolds. Conversely, ASB-14 5% scaffolds had a statistically increased fold-change in humoral response compared to GFBP scaffolds. The predominant difference in pre-implantation antigen content between ASB-14 5% and ASB-16 3% groups is the number of lipophilic antigens removed. ASB-16 3% removed 13% more lipophilic antigens than ASB-14 5% (79% versus 92% removal respectively). Furthermore, since the hydrophilic antigenicity of both scaffolds was not statistically different (95% for ASB-14 5% and 96% for ASB-16 3%), we conclude that reduction of hydrophile antigenicity alone is insufficient to overcome graft-specific humoral response. Indeed, this finding is supported by previous work, which demonstrated that removal of hydrophilic antigens only resulted in increased cell-mediated and humoral immune response compared to removal of both hydrophilic and lipophilic antigens[13]. Importantly, the present study demonstrates that ASB-16 at an optimal concentration of 3%, in the absence of magnesium chloride, is essential to overcome both hydrophilic and lipophilic antigen mediated graft-specific humoral responses [20,21,38].

Consequently, we conclude that the humoral immune response was more sensitive to residual antigenicity than is the cell-mediated response. Furthermore, a threshold level of at least 96% hydrophilic and 92% lipophilic antigen removal is necessary to reduce humoral response to levels comparable to GFBP.

Achieving the stringent immunologic threshold required to overcome recipient graft-specific adaptive immune responses requires exacting processes, which must also avoid inducing off-target damage to the remaining ECM components. Previous reports have demonstrated that disruption of ECM components following decellularization/antigen removal processes has potential to result in innate immune system activation [6,26,32,41], resulting in fibrous encapsulation and foreign body response [18,33,42]. In the current study, GFBP implants resulted in marked innate immune activation and resultant fibrous encapsulation. Both native and GFBP scaffolds exhibited a focal mononuclear cell response at the periphery of the scaffolds, which other literature has identified as indication of end-stage inflammatory response [5,42]. Such a reaction is normally present in a foreign body response where the host environment confines the graft tissue [5,42]. Indeed, in the current study, both native and GFBP scaffolds were associated with macrophage infiltration and resultant fibrosis and subsequent necrosis of the biomaterial [43,44]. Previous publications have noted that glutaraldehyde-fixed bovine pericardium underwent similar fibrosis and inflammatory responses [5,29]. Furthermore, it is generally accepted that toxicity leached by glutaraldehyde fixation inhibits recellularization and endothelialization [6,7]. More so, the irreversible crosslinks of proteins prevents cellular remodeling [18]. Non-immune cell

infiltration was minimal in either native or GFBP scaffold, and indeed central necrosis of both scaffold types was noted. This was most likely due to the foreign body response and a resultant inability for the scaffolds to undergo constructive remodeling [12,45,46].

By comparison both ASB-14 5% and ASB-16 3% showed no evidence of innate immune mediated destruction. Additionally, ASB-14 5% and ASB-16 3% scaffolds had minimal to non-existent fibrotic encapsulation and no evidence of necrosis. This finding was achieved despite the alterations in collagen alignment induced by ASB-14 5%. Even though the collagen alignment and content changed in ASB-14 5%, macromolecular structure, as assessed by DSC, was retained. This distinction suggests that the innate immune response is tolerant to minute deviations in ECM protein organization provided proteins are not denatured. Other literature also observed this phenomenon when examining the innate immune response to collagen denaturation [32,41,47]. For example, harsh decellularization methods (e.g., SDS) have been previously documented to result in significant ECM damage. Such alterations in composition, morphology, macromolecular structure and mechanical properties have been shown to induce innate immune mediated foreign body response, with marked fibrous encapsulation and central necrosis of scaffolds upon implantation [18,42,48]. Such studies, combined with the results of the current work, indicate that collagen macromolecular structure may be a better predictor of *in vivo* response to biomaterials than collagen content or collagen fibril alignment.

Scaffolds that avoid both adaptive and innate immune graft-specific destructive responses have potential for non-immune cell infiltration and constructive remodeling. ASB-14 5% and ASB-16 3% scaffolds both had spindle-shaped non-immune cells present throughout their scaffolds. Thampi et al. also observed non-immune cell infiltration through their decellularized bovine pericardial scaffolds, although their scaffolds were also accompanied by a mild to moderate presence of mononuclear immune cells [5]. The presence of spindle-shaped non-immune cells in ASB-14 5% and ASB-16 3% scaffolds potentially indicates a pro-regenerative response to the scaffolds. Based on polarized light microscopy, collagen alignment of ASB-16 3% decreased following *in vivo* implantation, indicating that the tissue is undergoing recipient cell-mediated remodeling [46]. Such alterations in collagen alignment post-implantation were not observed for ASB-14 5% scaffolds, despite non-immune cell infiltration, which may indicate that *in vitro* alterations in collagen alignment induced in this scaffold type may slow or prevent recipient cellular remodeling. Taken together, these results indicate that ASB-16 3% scaffolds represent an immunologically-acceptable xenogeneic biomaterial that undergoes pro-regenerative host repopulation and remodeling response.

5. Conclusion

This study established that at least 92% removal of lipid antigens is the threshold level of removed antigenicity necessary to overcome recipient graft-specific adaptive humoral immune response. We further identified that the graft-specific humoral adaptive immune response is more sensitive to ECM scaffold residual antigen content than is the cell-mediated response, providing critical information which should be utilized in future *in vivo* ECM scaffold studies. Furthermore, although proteomics is making vast strides in developing

compounds for enhancing protein solubilization, this study demonstrates that a detergent's capacity to solubilize proteins does not correlate with its ability to reduce the antigenic content of intact ECM scaffolds. Preserving the precarious balance between reducing residual antigenicity in xenogeneic tissue while maintaining native tissue biocompatibility and mechanics, has long been an obstacle in decellularization methods. Here we demonstrate that some ECM damage may be tolerated by the innate immune response, provided that macro-molecular structure is maintained. ASB-16 can not only solubilize and remove challenging lipophilic antigens from intact bovine pericardium, but in doing so, maintain the ECM structure and function of the native xenogeneic tissue. Ultimately, xenogeneic bovine pericardium that has undergone antigen removal using ASB-16 is tolerated by the innate immune response and overcomes the adaptive immune response; preserving recellularization capacity and demonstrating constructive remodeling. Therefore, a scaffold developed using ASB-16 3% may prove to be an ideal candidate material for use in bioprosthetic heart valve prostheses. Future studies are necessary to determine how scaffolds developed using ASB-16 3% perform in a heart valve leaflet configuration in a large animal model (e.g., ovine or porcine).

Supplementary Material

Refer to Web version on PubMed Central for supplementary material.

Acknowledgements

The authors would like to acknowledge funding from the National Institutes of Health (NIH R01HL115205). Additionally, the authors would like to thank the laboratory of Dr. Peter Moore (University of California, Davis, Davis, CA) for the generous use of $CD3^+$ primary antibody, Dr. Ronald Marler for his services as a board certified veterinary pathologist and Katherine Gates for her assistance in animal handling.

References

[1]. Iung B, Vahanian A, Epidemiology of acquired valvular heart disease, Can. J. Cardiol 30 (9) (2014) 962–970. [PubMed: 24986049]

[2]. Bloomfield P, Choice of heart valve prosthesis, Heart 87 (6) (2002) 583–589. [PubMed: 12010950]

[3]. Crapo PM, Gilbert TW, Badylak SF, An overview of tissue and whole organ decellularization processes, Biomaterials 32 (12) (2011) 3233–3243. [PubMed: 21296410]

[4]. Gates KV, Dalgliesh AJ, Griffiths LG, Antigenicity of bovine pericardium determined by a novel immunoproteomic approach, Sci. Rep 7 (1) (2017) 2446. [PubMed: 28550302]

[5]. Thampi P, Nair D, R L, N V, Venugopal S, Ramachandra U, Pathological effects of processed bovine pericardial scaffolds-a comparative in vivo evaluation, Artif. Organs 37 (7) (2013) 600–605. [PubMed: 23452255]

[6]. Chang Y, Tsai CC, Liang HC, Sung HW, In vivo evaluation of cellular and acellular bovine pericardia fixed with a naturally occurring crosslinking agent (genipin), Biomaterials 23 (12) (2002) 2447–2457. [PubMed: 12033592]

[7]. Huang-Lee LL, Cheung DT, Nimni ME, Biochemical changes and cytotoxicity associated with the degradation of polymeric glutaraldehyde derived crosslinks, J. Biomed. Mater. Res 24 (9) (1990) 1185–1201. [PubMed: 2120238]

[8]. Manji RA, Ekser B, Menkis AH, Cooper DK, Bioprosthetic heart valves of the future, Xenotransplantation 21 (1) (2014) 1–10. [PubMed: 24444036]

[9]. Platt J, DiSesa V, Gail D, Massicot-Fisher J, National Heart L, Blood Institute H, Lung G, Xenotransplantation working, recommendations of the national heart, lung, and blood institute

heart and lung xenotransplantation working group, Circulation 106 (9) (2002) 1043–1047. [PubMed: 12196325]

[10]. Badylak SF, The extracellular matrix as a biologic scaffold material, Biomaterials 28 (25) (2007) 3587–3593. [PubMed: 17524477]

[11]. Keane TJ, Badylak SF, The host response to allogeneic and xenogeneic biological scaffold materials, J. Tissue Eng. Regen. Med 9 (5) (2015) 504–511. [PubMed: 24668694]

[12]. Londono R, Badylak SF, Biologic scaffolds for regenerative medicine: mechanisms of in vivo remodeling, Ann. Biomed. Eng 43 (3) (2015) 577–592. [PubMed: 25213186]

[13]. Wong ML, Wong JL, Vapniarsky N, Griffiths LG, In vivo xenogeneic scaffold fate is determined by residual antigenicity and extracellular matrix preservation, Biomaterials 92 (2016) 1–12. [PubMed: 27031928]

[14]. Gates KV, Dalgliesh AJ, Griffiths LG, Antigenicity of bovine pericardium determined by a novel immunoproteomic approach, Sci. Rep 7 (2017).

[15]. Cascalho M, Platt JL, The immunological barrier to xenotransplantation, Immunity 14 (4) (2001) 437–446. [PubMed: 11336689]

[16]. Simon P, Kasimir MT, Seebacher G, Weigel G, Ullrich R, Salzer-Muhar U, Rieder E, Wolner E, Early failure of the tissue engineered porcine heart valve SYNERGRAFT in pediatric patients, Eur. J. Cardiothorac. Surg 23 (6) (2003) 1002–1006. discussion 1006. [PubMed: 12829079]

[17]. Daly KA, Stewart-Akers AM, Hara H, Ezzelarab M, Long C, Cordero K, Johnson SA, Ayares D, Cooper DK, Badylak SF, Effect of the alphaGal epitope on the response to small intestinal submucosa extracellular matrix in a nonhuman primate model, Tissue Eng. Part A 15 (12) (2009) 3877–3888. [PubMed: 19563260]

[18]. Hulsmann J, Grun K, El Amouri S, Barth M, Hornung K, Holzfuss C, Lichtenberg A, Akhyari P, Transplantation material bovine pericardium: biomechanical and immunogenic characteristics after decellularization vs. glutaraldehyde-fixing, Xenotransplantation 19 (5) (2012) 286–297. [PubMed: 22978462]

[19]. Kasimir MT, Rieder E, Seebacher G, Wolner E, Weigel G, Simon P, Presence and elimination of the xenoantigen gal (alpha1, 3) gal in tissue-engineered heart valves, Tissue Eng. 11 (7–8) (2005) 1274–1280. [PubMed: 16144463]

[20]. Wong ML, Wong JL, Athanasiou KA, Griffiths LG, Stepwise solubilization-based antigen removal for xenogeneic scaffold generation in tissue engineering, Acta Biomater. 9 (5) (2013) 6492–6501. [PubMed: 23321301]

[21]. Wong ML, Leach JK, Athanasiou KA, Griffiths LG, The role of protein solubilization in antigen removal from xenogeneic tissue for heart valve tissue engineering, Biomaterials 32 (32) (2011) 8129–8138. [PubMed: 21810537]

[22]. Rabilloud T, Solubilization of proteins in 2DE: an outline, Methods Mol. Biol 519 (2009) 19–30. [PubMed: 19381574]

[23]. Henningsen R, Gale BL, Straub KM, DeNagel DC, Application of zwitterionic detergents to the solubilization of integral membrane proteins for two-dimensional gel electrophoresis and mass spectrometry, Proteomics 2 (11) (2002) 1479–1488. [PubMed: 12442247]

[24]. Rabilloud T, Gianazza E, Catto N, Righetti PG, Amidosulfobetaines, a family of detergents with improved solubilization properties: application for isoelectric focusing under denaturing conditions, Anal. Biochem 185 (1) (1990) 94–102. [PubMed: 2344051]

[25]. Keane TJ, Swinehart IT, Badylak SF, Methods of tissue decellularization used for preparation of biologic scaffolds and in vivo relevance, Methods 84 (2015) 25–34. [PubMed: 25791470]

[26]. Keane TJ, Londono R, Turner NJ, Badylak SF, Consequences of ineffective decellularization of biologic scaffolds on the host response, Biomaterials 33 (6) (2012) 1771–1781. [PubMed: 22137126]

[27]. N.I.o. Health, Guide for the Care and Use of Laboratory Animals, in: C.f.t.U.o.t.G. f.t.C.a.U.o.L. Animals (Ed.) The National Academies Press, Washington, D.C., 2011.

[28]. McPherson TB, Liang H, Record RD, Badylak SF, Galalpha(1,3)Gal epitope in porcine small intestinal submucosa, Tissue Eng. 6 (3) (2000) 233–239. [PubMed: 10941218]

[29]. Manji RA, Zhu LF, Nijjar NK, Rayner DC, Korbutt GS, Churchill TA, Rajotte RV, Koshal A, Ross DB, Glutaraldehyde-fixed bioprosthetic heart valve conduits calcify and fail from xenograft rejection, Circulation 114 (4) (2006) 318–327. [PubMed: 16831988]

[30]. Griffiths LG, Choe LH, Reardon KF, Dow SW, Christopher Orton E, Immunoproteomic identification of bovine pericardium xenoantigens, Biomaterials 29 (26) (2008) 3514–3520. [PubMed: 18514307]

[31]. Luche S, Santoni V, Rabilloud T, Evaluation of nonionic and zwitterionic detergents as membrane protein solubilizers in two-dimensional electrophoresis, Proteomics 3 (3) (2003) 249–253. [PubMed: 12627377]

[32]. Hwang J, San BH, Turner NJ, White LJ, Faulk DM, Badylak SF, Li Y, Yu SM, Molecular assessment of collagen denaturation in decellularized tissues using a collagen hybridizing peptide, Acta Biomater. 53 (2017) 268–278. [PubMed: 28161576]

[33]. Gratzer PF, Harrison RD, Woods T, Matrix alteration and not residual sodium dodecyl sulfate cytotoxicity affects the cellular repopulation of a decellularized matrix, Tissue Eng. 12 (10) (2006) 2975–2983. [PubMed: 17518665]

[34]. Faulk DM, Wildemann JD, Badylak SF, Decellularization and cell seeding of whole liver biologic scaffolds composed of extracellular matrix, J. Clin. Exp. Hepatol 5 (1) (2015) 69–80. [PubMed: 25941434]

[35]. Liu ZZ, Wong ML, Griffiths LG, Effect of bovine pericardial extracellular matrix scaffold niche on seeded human mesenchymal stem cell function, Sci. Rep 6 (2016) 37089. [PubMed: 27845391]

[36]. D'Andrea MG, Domingues CC, Malheiros SV, Neto FG, Barbosa LR, Itri R, Almeida FC, de Paula E, Bianconi ML, Thermodynamic and structural characterization of zwitterionic micelles of the membrane protein solubilizing amidosulfobetaine surfactants ASB-14 and ASB-16, Langmuir 27(13) (2011) 8248–8256. [PubMed: 21657261]

[37]. Rabilloud T, Protein solubility in two-dimensional electrophoresis, in: Walker J (Ed.), The Protein Protocols Handbook, Humana Press, Totowa, 2002, pp. 78–79.

[38]. Dalgliesh AJ, Liu ZZ, Griffiths LG, Magnesium presence prevents removal of antigenic nuclear-associated proteins from bovine pericardium for heart valve engineering, Tissue Eng. Part A 23 (13–14) (2017) 609–621. [PubMed: 28178887]

[39]. Dahm M, Lyman WD, Schwell AB, Factor SM, Frater RW, Immunogenicity of glutaraldehyde-tanned bovine pericardium, J. Thorac. Cardiovasc. Surg 99(6) (1990) 1082–1090. [PubMed: 2141662]

[40]. Human P, Zilla P, Characterization of the immune response to valve bioprostheses and its role in primary tissue failure, Ann. Thorac. Surg 71 (5 Suppl) (2001) S385–S388. [PubMed: 11388230]

[41]. Glimcher MJ, Mechanism of calcification: role of collagen fibrils and collagen-phosphoprotein complexes in vitro and in vivo, Anat. Rec 224 (2) (1989) 139–153. [PubMed: 2672881]

[42]. Anderson JM, Rodriguez A, Chang DT, Foreign body reaction to biomaterials, Semin. Immunol 20 (2) (2008) 86–100. [PubMed: 18162407]

[43]. Badylak SF, Valentin JE, Ravindra AK, McCabe GP, Stewart-Akers AM, Macrophage phenotype as a determinant of biologic scaffold remodeling, Tissue Eng. Part A 14 (11) (2008) 1835–1842. [PubMed: 18950271]

[44]. Jorge-Herrero E, Fonseca C, Barge AP, Turnay J, Olmo N, Fernandez P, Lizarbe MA, Garcia Paez JM, Biocompatibility and calcification of bovine pericardium employed for the construction of cardiac bioprostheses treated with different chemical crosslink methods, Artif. Organs 34 (5) (2010) E168–E176. [PubMed: 20633147]

[45]. Valentin JE, Stewart-Akers AM, Gilbert TW, Badylak SF, Macrophage participation in the degradation and remodeling of extracellular matrix scaffolds, Tissue Eng. Part A 15 (7) (2009) 1687–1694. [PubMed: 19125644]

[46]. Brown BN, Valentin JE, Stewart-Akers AM, McCabe GP, Badylak SF, Macrophage phenotype and remodeling outcomes in response to biologic scaffolds with and without a cellular component, Biomaterials 30 (8) (2009) 1482–1491. [PubMed: 19121538]

[47]. Wang Y, Azais T, Robin M, Vallee A, Catania C, Legriel P, Pehau-Arnaudet G,Babonneau F, Giraud-Guille MM, Nassif N, The predominant role of collagen in the nucleation, growth,

structure and orientation of bone apatite, Nat. Mater 11 (8) (2012) 724–733. [PubMed: 22751179]

[48]. Junge K, Binnebosel M, von Trotha KT, Rosch R, Klinge U, Neumann UP, Lynen Jansen P, Mesh biocompatibility: effects of cellular inflammation and tissue remodelling, Langenbecks Arch. Surg 397 (2) (2012) 255–270. [PubMed: 21455703]

Statement of Significance

Removal of antigenic components from candidate xenogeneic biomaterials is the primary success criteria for development of extracellular matrix (ECM) scaffolds in tissue engineering applications. Currently, the threshold level of residual biomaterial antigenicity required to overcome recipient graft-specific adaptive immune responses is unknown. Additionally, the extent to which the innate immune response tolerates changes to the native ECM, resulting from the ECM scaffold production process, has yet to be determined. This manuscript not only establishes the threshold for tolerable residual antigenicity, but also demonstrates that deviations in protein organization are tolerated by the innate immune system, provided macromolecular structure remains intact. In doing so, we provide the foundation of an immunologically-acceptable unfixed xenogeneic biomaterial for use in clinical applications.

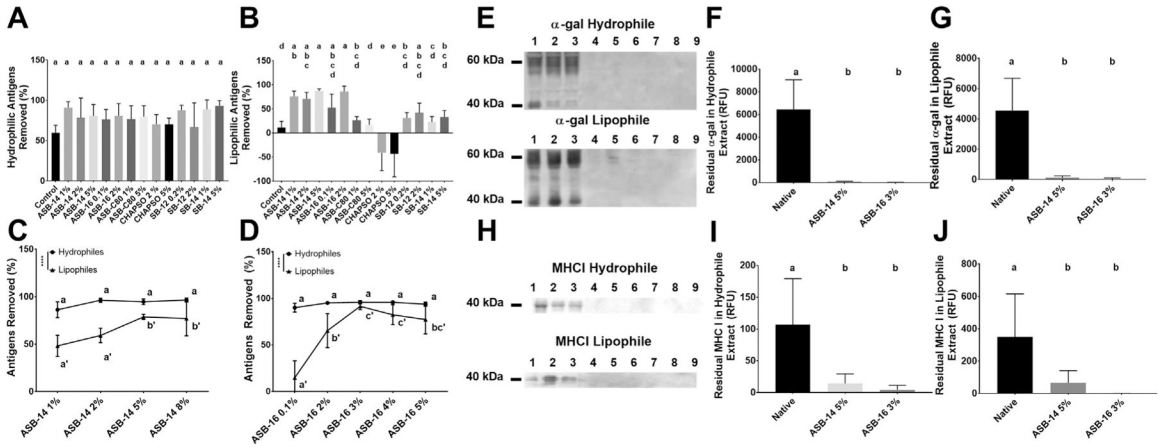

Fig. 1.

Specific sulfobetaine compound and concentration are critical factors in removal of antigens from bovine pericardium. Six different sulfobetaine compounds within a range of concentrations were assessed for their effect on hydrophilic (A) and lipophilic (B) antigen removal. Neither specific sulfobetaine, nor concentration used, altered hydrophilic antigen removal (A). Lipophilic antigen removal, however, was dependent on specific sulfobetaine used, with ASB-14 and ASB-16 removing the greatest amount of lipophilic antigens (B). Both ASB-14 (C) and ASB-16 (D) showed concentration dependent effect on lipophilic antigen removal, which plateaued at 5% for ASB-14 and peaked at 3% for ASB-16. On western blotting marked reduction in residual α-gal (G) and MHCI (H) for both ASB-14 5% (lanes 4–6) and ASB-16 3% (lanes 7–9) scaffolds compared to native extract (lanes 1–3) was visualized. Quantification of residual known antigens demonstrated a significant reduction in both the hydrophile and lipophile extracts of α-gal (F and G respectively), as well as MHCI (I and J respectively) when ASB-14 5% and ASB-16 3% were used compared to native tissue. $n = 6$ per group. Groups not connected by the same lower case letter are statistically significantly different. For figures ASB-14 (C) and ASB-16 (D), statistical significance is represented in lower case (hydrophile extract) and lower case with apostrophe (lipophile extract). All data represent the mean ± s.d.

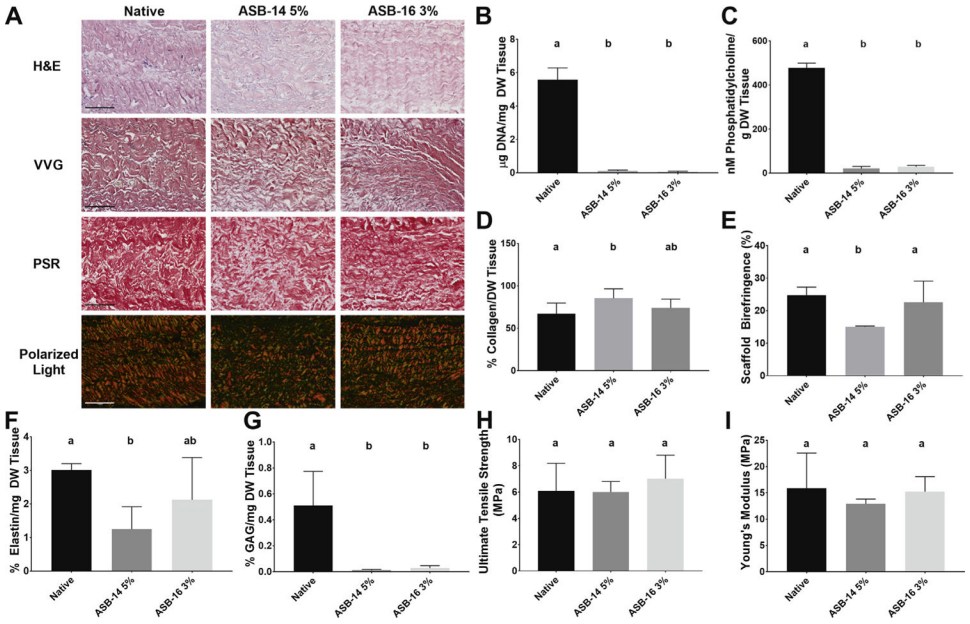

Fig. 2.

Use of ASB-14 5% and ASB-16 3% achieved complete decellularization, although preservation of native ECM structure, composition, and function was superior for ASB-16 3% scaffolds. Scaffolds treated with ASB-14 5% and ASB-16 3% underwent ualitative histological analysis to assess nuclei presence and ECM morphology (H&E), elastin content and morphology (VVG) and collagen content and alignment (PSR and polarized light respectively) (A). Both ASB-14 5% and ASB-16 3% statistically decreased DNA (B) and phosphatidylcholine (C) content compared to native. However, ASB-14 5% also statistically decreased collagen content (D) and collagen alignment (E), as well as elastin content (F), whereas ASB-16 3% did not. Both ASB-14 5% and ASB-16 3% statistically removed glycosaminoglycans (G) compared to native tissue. Both ultimate tensile strength (H) and Young's Modulus (I) were maintained compared to native tissue. Scale bar represents 100 μm and $n = 6$ per group. Groups not connected by the same lower case letter are statistically significantly different. Data represent the mean ± s.d.

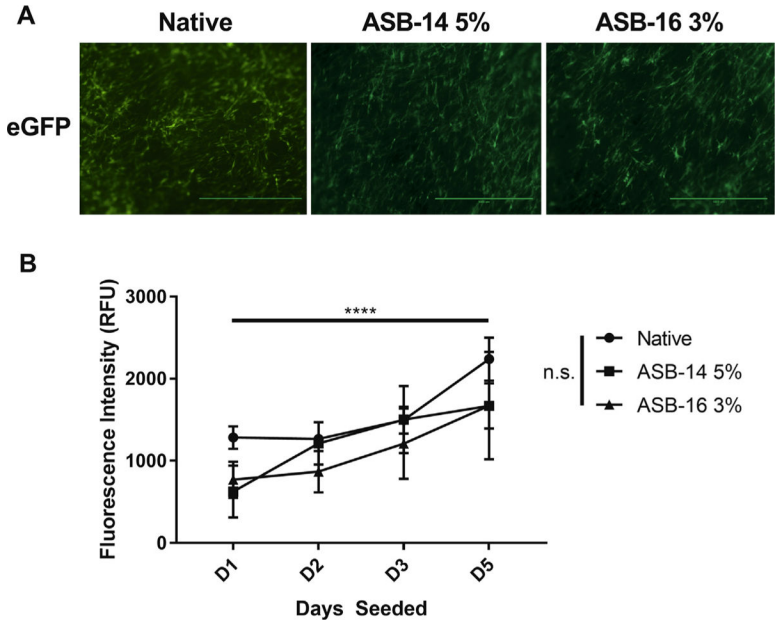

Fig. 3.

Recellularization capacity was maintained in scaffolds following antigen removal using ASB-14 5% and ASB-16 3% when compared to native tissue. eGFP labeled human mesenchymal stem cells (hMSCs) were imaged at 40x magnification and showed no qualitative difference in recellularization capacity or cell morphology between antigen removed scaffolds and native tissue (A). Cytotoxicity and cellular viability were quantified using Alamar Blue at Day 1, Day 2, Day 3 and Day 5 (B). There was no statistical difference in cell viability or cytotoxicity between antigen removed scaffolds and native tissue. All groups demonstrated increasing cell numbers over time. Scale bar represents 1000 μm and n = 4 per group. All data. represent the mean ± s.d.

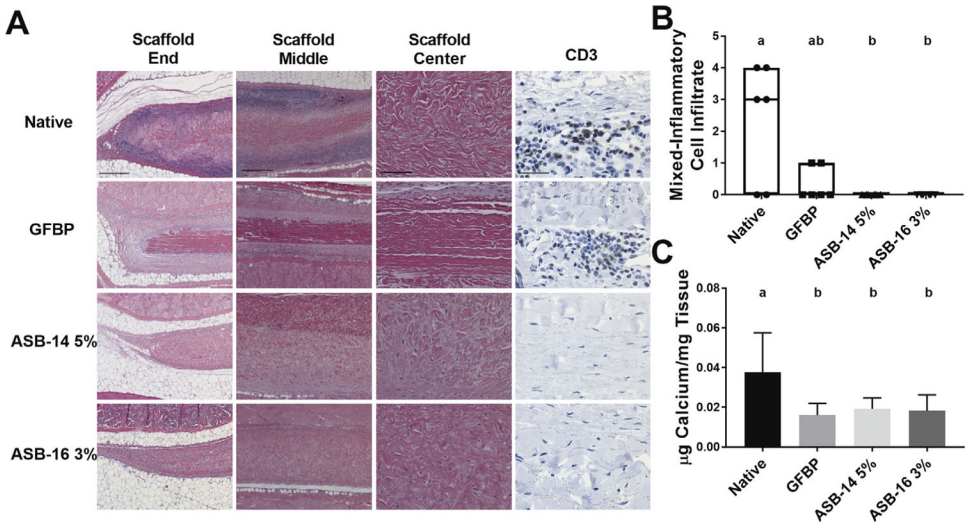

Fig. 4.

Antigen removal significantly reduced recipient graft-specific cell-mediated adaptive immune response. Representative H&E stained histological images of the end (100×), middle (100×), and center (200×) of explanted scaffolds (A). Native bovine pericardium resulted in robust cell-mediated adaptive response (lymphocytes in dark purple regions) at both the end and middle of the scaffold. Lymphocytic infiltration was reduced in glutaraldehyde-fixed bovine pericardium (GFBP) compared to native tissue, although still present at the scaffold ends. Conversely, lymphocytic infiltration was absent in all locations for either ASB-14 5% or ASB-16 3% scaffolds (A). CD3 staining (400×) confirmed that cells observed on H&E staining are lymphocytes and further demonstrated absence of cell-mediated response towards ASB-14 5% or ASB-16 3% scaffolds (A). Blinded review of H&E images by a board certified veterinary pathologist categorized inflammatory cell infiltration on a semi-quantitative scale and confirmed that native tissue stimulated significantly more immune cell response than ASB-14 5% or ASB- 16 3% (B). Calcium deposition was significantly greater in native bovine pericardium explants than in GFBP, ASB-14 5%, and ASB-16 3% (C). Scale bar represents 500 μm (scaffold end and middle images), 100 μm (scaffold center), and 100 μm (CD3). $n = 6$ per group. Groups not connected by the same lower case letter are statistically significantly different. All data represent the mean ± s.d. except pathology results, which were plotted as median (denoted by the thick line), inter-quartile range (25th–75th percentile), maximum (top whisker) and minimum (bottom whisker).

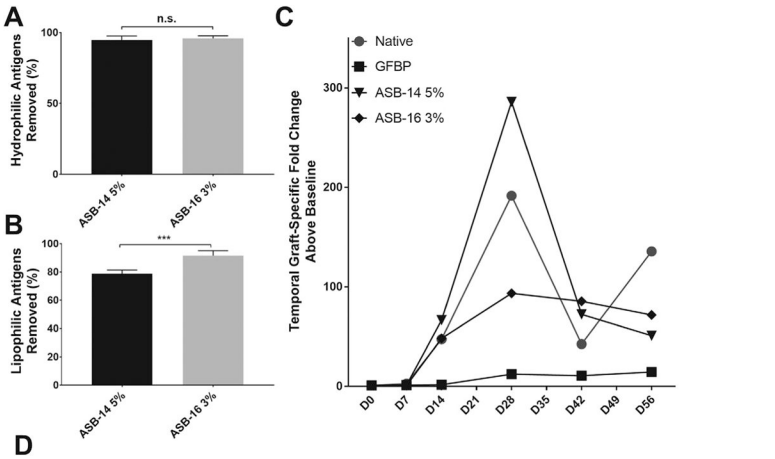

D

Scaffold	D0	D7	D14	D28	D42	D56	
Native	1 ± 0	2.8 ± 2.0	47.3 ± 22.3	191.6 ± 101.8	42.5 ± 18.3	135.7 ± 94.9	a
GFBP	1 ± 0	1.3 ± 0.5	1.7 ± 0.5	21.4 ± 15.5	10.8 ± 8.5	14.5 ± 7.3	b
ASB-14 5%	1 ± 0	1.4 ± 0.5	66.5 ± 57.0	286.1 ± 82.0	72.3 ± 25.5	50.9 ± 26.2	a
ASB-16 3%	1 ± 0	0.83 ± 0.06	48.2 ± 34.7	93.5 ± 17.6	85.4 ± 55.4	71.7 ± 56.6	ab
	c'	c'	b'	a'	b'	b'	

Fig. 5.

Significant reduction in recipient graft-specific humoral adaptive immune response was only achieved when a threshold level of lipophilic antigens are removed. Both ASB-14 5% and ASB-16 3% removed >95% of hydrophilic antigens (A). However, ASB-16 3% removed significantly more lipophilic antigens (92%) than did ASB-14 5% (79%) (B). Graftspecific antibody production towards native pericardium peaked at 28 days post-implantation for all groups (C). Graft-specific antibody response towards scaffolds generated using ASB-14 5% was unaltered compared to native tissue, whereas ASB-16 3% scaffolds reduced graft-specific antibody production (C). Graft-specific antibody production towards ASB-16 3% was not significantly different from GFBP (negative humoral immune response control) (D). $n = 6$ per group. Groups not connected by the same lower case letter are statistically significantly different. For fold-change in antibody production (D), statistical significance is represented in lower case (group) and lower case with apostrophe (day). All data represent mean ± s.d.

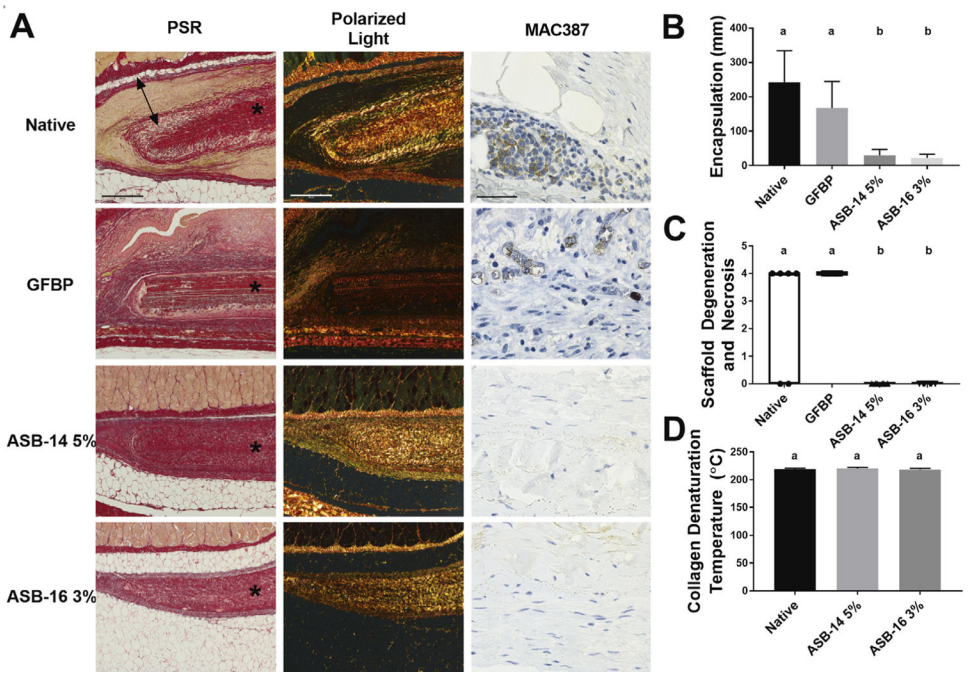

Fig. 6.

Alterations in collagen organization are tolerated if molecular structure remains intact. Representative histologic images of PSR, polarized light, and MAC387 (macrophage) staining of explanted scaffolds (A). All images are oriented with the panniculus muscle (skin side) at the top of the image. * denotes scaffold, double headed arrow denotes fibrous encapsulation. Fibrotic encapsulation around the implants was extensive for native and glutaraldehyde-fixed bovine pericardium (GFBP) scaffolds, but not ASB-14 5% or ASB-16 3% (B). Blinded review of H&E images by a board certified veterinary pathologist categorized scaffold degeneration and necrosis using a semi-quantitative scale (C). Native and GFBP scaffolds stimulated significantly more scaffold degeneration and necrosis than either ASB-14 5% or ASB-16 3% scaffolds. ASB-14 5% and ASB-16 3% scaffolds universally exhibited evidence of integration with recipient tissues as indicated by degeneration and necrosis score of 0 and lack of fibrosis. Native ECM collagen macromolecular structure (denaturation temperature) was preserved in both ASB-14 5% and ASB-16 3% scaffolds (D). Scale bar represents 500 μm (PSR and polarized light) and 50 μm (MAC387). $n = 6$ per group. Groups not connected by the same lower case letter are statistically significantly different. All data represent the mean ± s.d. except pathology results, which were plotted as median (denoted by the thick line), inter-quartile range (25th–75th percentile), maximum (top whisker) and minimum (bottom whisker).

Table 1

Individual sulfobetaines and concentrations used for lipophilic antigen removal from bovine pericardium.

Sulfobetaine	Concentration
Amidosulfobetaine-14	1%, 2%, 5%, 8%
Amidosulfobetaine-16 *	0.1%, 2%, 3%, 4%, 5%
Amidosulfobetaine-C80	1%, 5%
CHAPSO	2%, 5%
Sulfobetaine-12 *	0.2%, 2%
Sulfobetaine-14 *	1%, 5%

* Detergents purchased from G-Biosciences, St. Louis, MO.

Table 2

Semi-quantitative histologic scoring scheme for leporine local cellular response to implanted bovine pericardium scaffolds.

Score	Encapsulation and fibroplasia	Inflammatory cell infiltrate (Mixed)	Degeneration and necrosis
0	No fibrotic encapsulation	No presence of immune cells	Full infiltration of non-immune cells
1	Mild fibrotic encapsulation	Mild peripherallymphocyt presence	Moderate infiltration of non- immune cells
2	Moderate fibrotic encapsulation	Moderate lymphocyte presence	Some peripheral presence of non- immune cells
3	Severe fibrotic encapsulation	Severe infiltration of lymphocytes	Absence of cells in scaffold central area and degeneration of collagen
4	Foreign body response with giant cell presence and severe fibrotic encapsulation	Severe infiltration of lymphocytes and lymphocytic follicle formation	Absence of cells and degeneration of collagen throughout scaffold

Table 3

Graft-specific antibody production towards ASB-16 3% was not significantly different from GFBP.

Scaffold	D0	D7	D14	D28	D42	D56	
Native	1±0	2.8 ± 2.0	47.3 ± 22.3	191.6 ± 101.8	42.5 ± 18.3	135.7 ± 94.9	a
GFBP	1±0	1.3±0.5	1.7 ± 0.5	21.4±15.5	10.8±8.5	14.5 ± 7.3	b
ASB-14 5%	1±0	1.4±0.5	66.5 ± 57.0	286.1 ± 82.0	72.3 ±25.5	50.9 ± 26.2	a
ASB-16 3%	1±0	0.83 ± 0.06	48.2 ± 34.7	93.5 ± 17.6	85.4 ± 55.4	71.7 ±56.6	ab
	c’	c’	b’	a’	b’	b’	

Acta Biomater. Author manuscript; available in PMC 2019 October 01.